Polymer 192 (2020) 122308

Contents lists available at ScienceDirect

Polymer

journal homepage: http://www.elsevier.com/locate/polymer

Investigating the atmospheric pressure plasma jet modification of a photo-crosslinkable hydrogel

Inès Hamouda [a,b,c], Cédric Labay [a,b,c], Maria Pau Ginebra [a,b,c,d], Erwan Nicol [e,**], Cristina Canal [a,b,c,*]

[a] Biomaterials, Biomechanics and Tissue Engineering Group, Dpt. Materials Science and Metallurgy, Technical University of Catalonia (UPC), c. Eduard Maristany 10-14, 08019, Barcelona, Spain
[b] Barcelona Research Center in Multiscale Science and Engineering, UPC, Barcelona, Spain
[c] Research Centre for Biomedical Engineering (CREB), UPC, Barcelona, Spain
[d] Institute for Bioengineering of Catalonia, c/ Baldiri i Reixach 10-12, 08028, Barcelona, Spain
[e] Institut des Molécules et Matériaux du Mans, UMR-CNRS 6283, Le Mans Université, Avenue Olivier Messiaen, 72085, Le Mans cedex 9, France

ARTICLE INFO

Keywords:
Atmospheric pressure plasma jet
Photo-crosslinking
Polymer solution
Hydrogel
Self-assembly

ABSTRACT

Atmospheric pressure plasma jets (APPJ) have great potential in wound healing, bacterial disinfection and in cancer therapy. Recent studies pointed out that hydrogels can be used as screens during APPJ treatment, or even be used as reservoirs for reactive oxygen and nitrogen species generated by APPJ in liquids. Thus, novel applications are emerging for hydrogels which deserve fundamental exploration of the possible modifications undergone by the polymers in solution due to the reactivity with plasmas. Here we investigate the possible modifications occurred by APPJ treatment of an amphiphilic poly(ethylene oxide)-based triblock copolymer (tPEO) photo-crosslinkable hydrogel. While APPJ treatments lead to a certain degradation of the self-assembly of the polymeric chains at low concentrations (<2 g/L), at the higher concentrations required to form a hydrogel (>2 g/L), the polymeric chains are unaffected by APPJ and the hydrogel forming ability is kept. APPJ treatments induced a pre-crosslinking of the network with an increase of the mechanical properties of the hydrogel. Overall, the small modifications induced allow thinking of polymer solutions with hydrogel forming ability a new platform for several applications related to plasma medicine, and thus, with potential in different therapies.

1. Introduction

Research dealing with cold plasma modification of polymers has traditionally employed polymers in the solid state to alter parameters such as adhesion, wettability, etc., usually employing low pressure plasma processes [1]. Chemical processes on the surface of polymers take place through all major plasma components, namely electrons, ions, excited particles, radicals, atoms and UV radiation. The major primary products of treatment of polymer films with plasma are free radicals, non-saturated organic compounds, cross-links between polymer macromolecules, products of destruction of the polymer chains, and gas phase products. Most processes for the formation of radicals on the polymer surface under plasma treatment are due to electron impact and UV radiation and are related to breaking of R–H and C–C bonds in macromolecules. The main effects derived from these processes can be linked to functionalization and etching [2].

Nevertheless, with the development of Atmospheric Pressure Plasma Jets (APPJ) [3–11], which operate at near ambient temperature and atmospheric pressure a range of new possibilities has opened. For instance, in the last few years, APPJ treatment of polymeric solutions has been investigated to improve their printability by electro-spinning [12–14]. More recently, alginate solutions [15] have shown the ability of generating reactive species following APPJ treatment and still form stable hydrogels, opening great perspectives in the design of new implantable biomaterials for plasma therapies. In parallel, agarose and gelatin semi-solid hydrogels have been investigated by Szili et al. [16–18] in order to mimic the effects of plasmas through the skin, and evaluate the transport of reactive oxygen and nitrogen species (RONS)

* Corresponding author. Biomaterials, Biomechanics and Tissue Engineering Group, Dpt. Materials Science and Metallurgy, Technical University of Catalonia (UPC), c. Eduard Maristany 10-14, 08019, Barcelona, Spain.
** Corresponding author.
E-mail addresses: erwan.nicol@univ-lemans.fr (E. Nicol), cristina.canal@upc.edu (C. Canal).

https://doi.org/10.1016/j.polymer.2020.122308
Received 4 November 2019; Received in revised form 7 February 2020; Accepted 18 February 2020
Available online 21 February 2020

from the plasma gas phase to investigate them as screens for certain species from APPJ during treatment of living tissues. Although the complete mechanisms involved in the biological effects of plasma treatment are not yet fully understood, APPJ devices present a safe, versatile and easy application without inducing heating to the treated living or non-living surfaces at short treatment times [10,19–21]. The efficiency of these plasma therapies is essentially related to the generation of RONS in biological tissues or liquids [22–24].

Thus, the variety of applications emerging in this area foster the interest for fundamental investigation of the effects of APPJ on polymer solutions.

In this sense, the plasma chemistry occurring in liquids is completely different to that described earlier occurring in solid surfaces; as reported in a recent review [25], the transfer of reactivity from the gas to the liquid phase has been highlighted as being of prime importance for biological effects. In fact, plasma treatment of aqueous solutions (water, saline solutions, or cell culture media) leads to their activation and non-equilibrium dissociation of water molecules. This results in the formation of short-lived species such as H atoms, OH* radicals, and hydrated (solvated) electrons (e_{solv}). Very quick reactions between these species lead to the formation of transient and more stable species such as O_3, H_2, O_2, H_2O_2 etc. Moreover, in the presence of air, reactive nitrogen species (NO^-, NO_2^-, NO_3^-, $ONOO^-$) are also formed in liquid medium. These nitrogen oxides subsequently react in water forming acids, which affect the conductivity and pH of the plasma-treated liquids, and further reactions may occur.

As mentioned earlier, natural polymers (alginate, agarose, gelatin) have been treated by APPJ in solution or in hydrated hydrogel state for a variety of applications. To the best of our knowledge, the effects derived from the reactions between the cocktail of reactive species generated by APPJ and polymeric solutions are challenging and still largely unexplored. However, assessing certain modifications in natural polymers can be rather challenging, so it is of interest to employ a synthetic polymer with hydrogel-forming ability, that can be used as a first model to investigate the potential changes and reactivity undergone through APPJ treatment.

Among potential polymers that can be employed to form hydrogels, poly(ethylene glycol) (PEG) (also called poly(ethylene oxide) (PEO)), a biocompatible synthetic polymer, has good properties for tissue engineering and drug delivery applications [26–30], so it might also be of interest for the novel applications highlighted earlier. By introducing methacrylate functional end groups in the polymer chains, through adequate chemical modification, the polymeric solution can undergo photo-crosslinking in the presence of photo-initiators to form a self-standing hydrogel [31–35]. One of the major advantages of photo-crosslinked hydrogels is that they can be formed *in situ* in a minimally invasive manner.

A few years ago, we developed a PEO-based self-associating amphiphilic triblock copolymer (tPEO) able form injectable and rapidly photo-cross-linkable hydrogels [31]. Associated to other macromolecules, this copolymer can lead to microporous hydrogels [36] or double network hydrogels of enhanced mechanical properties [37,38]. It was also shown to be non-cytotoxic and biocompatible leading to potential biomedical applications (paper under preparation) . Therefore, we explore here the APPJ treatment of a photo-crosslinkable tPEO self-assembling polymer solution and analyze the potential modifications in the polymer (ie. self-assembly in micelles) through different techniques, including the conservation of the ability of the hydrogel photo-crosslinking, its mechanical properties and chemical modifications.

2. Materials and methods

2.1. Materials

Phosphate Buffered Saline (PBS) tablets were purchased from Gibco Life technologies. N-phenylglycine (NPG) (≥97% purity, M.W.: 151.16 g/mol, powder form), triethanolamine (TEA) (purity ≥ 99.0%, M.W.: 149.19 g/mol, liquid form), riboflavin (purity ≥ 98%, M.W.: 376.36 g/mol, powder form), dimethyl sulfoxide (purity ≥ 99.7%, M.W.: 78.13 g/mol, liquid form), sulphanilamide (purity ≥ 99%, M.W.: 172.20 g/mol, powder form), N-(1-naphtyl) ethylenediamine (NEED) (purity > 98%, M.W.: 172.20 g/mol; powder form). Ethanol (99.8% purity) and phosphoric acid (85%, M.W.: 98 g/mol, liquid form) were purchased from Panreac. All reagents were used as received in their chemical grade except for NPG, which was purified by dissolving in water at 60 °C, filtered over 0.45 μm filter then freeze-dried before use. Gaseous He for plasma treatments was purchased from PRAXAIR, Spain.

2.2. Polymer synthesis

Poly(2-methacryloyloxyethyl acrylate)-b-poly(ethylene oxide)-b-poly(2-methacryloyloxyethyl acrylate) ($PMEA_7$-b-PEO_{270}-b-$PMEA_7$) triblock copolymer (tPEO) was synthesized as reported elsewhere [39]. Each polymeric solution was prepared by dilution in PBS and homogenized overnight.

2.3. Hydrogel preparation

Hydrogels were prepared from a tPEO solution at 40 g/L in presence of N-phenylglycine (NPG), triethanolamine (TEA) and riboflavin as photo-initiating system (PIS) components. In a 10 mL glass bottle, 20 μL of purified NPG at 90 mg/mL in ethanol were introduced with 20 μL of TEA at 90 mg/mL in ethanol. Solvent was evaporated gently using compressed air before adding 2 mL of tPEO solution and stirring was performed overnight protected from light. Before crosslinking, 20 μL of riboflavin solution at a concentration of 28 mg/mL in dimethylsulfoxide were added. To obtain a photo-crosslinked hydrogel, 200 μL of sample were placed in a 48-well plate and irradiated during 3 min using blue light (LED light curing machine LY-C240, λ = 420–480 nm, I = 100 mW/cm^2) (Fig. 1).

2.4. Plasma treatment

An atmospheric pressure plasma jet (APPJ) using He as plasma carrier gas was employed, in a jet design with a single electrode described elsewhere [40]. Plasma discharge was operating with sinusoidal waveform at 25 kHz with (U) ~ 2 kV and (I) ~ 3 mA. Helium flow was regulated at 1 L/min through a Bronkhorst MassView (Bronkhorst, Netherlands) mass flow controller.

To treat liquids and polymer solutions with plasma, 2 mL of the corresponding sample was introduced in a 24-mm diameter glass bottle and plasma treatments were performed from 15 to 900 s, using a gap of 10 mm between plasma nozzle and the surface of the sample (Fig. 2). Due to water evaporation during plasma treatment, the concentration of the solution was recalculated after each APPJ treatment.

2.5. Light scattering

Apparent molar masses (Ma) and hydrodynamic radius (R_{ha}) of tPEO self-assemblies in solution were assessed by static (SLS) and dynamic (DLS) light scattering. Data were recorded with a ALV-5000 multibit (ALV-GmbH, Germany), multitau, full digital correlator in combination with a Spectra-Physics laser (emitting vertically polarized light at k = 632.8 nm) and a thermostat bath controlled within ±0.2 °C. Measurements were made at angles (θ) ranging between 20 and 150°. Before measurement, the polymer solutions were filtered using 0.2 μm inorganic membrane filter. Polymer concentration varied between 0.5 and 10 g/L and the refractive index increment of the copolymer in water was assumed to be that of pure PEO in water, i.e., (dn/dC) = 0.135 mL/g. The average relaxation rate (Γ) was found to be q^2 independent (where q is the scattering vector: $q = (4\pi n/k)/\sin(\theta/2)$). The cooperative diffusion coefficient (Dc) was calculated as: $Dc = \Gamma/q^2$. At sufficiently low

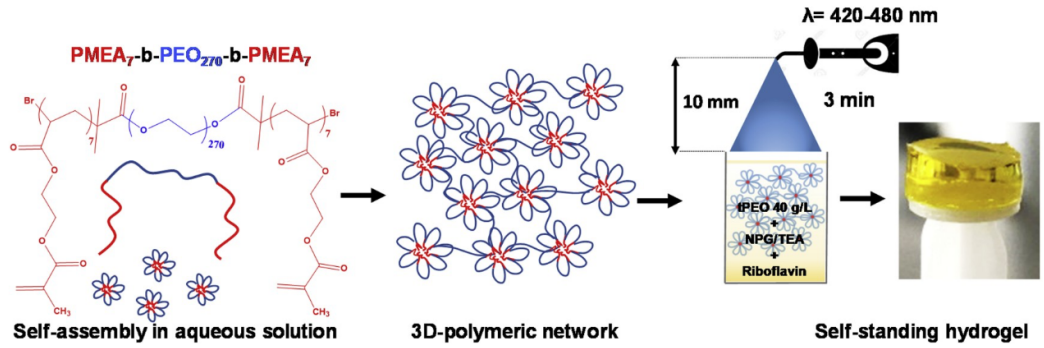

Fig. 1. Chemical structure, self-assembly in aqueous solutions of tPEO and its photo-crosslinking at 40 g/L using blue light. (For interpretation of the references to colour in this figure legend, the reader is referred to the Web version of this article.)

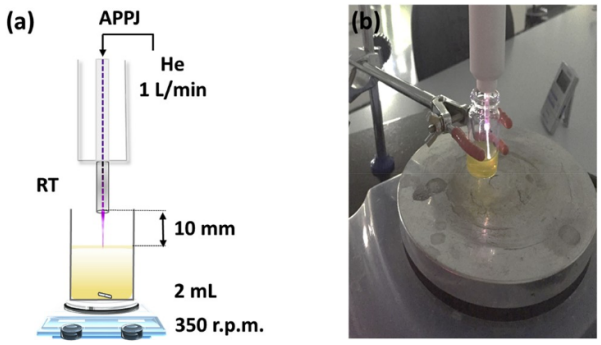

Fig. 2. (a) Scheme of the experimental setup of plasma treatment of samples; (b) Picture of plasma treatment of tPEO solution during plasma treatment.

concentrations, where interactions are negligible, the z-average apparent hydrodynamic radius (R_{ha}) of the solute can be calculated from the diffusion coefficient (Dc) using the Stokes-Einstein relation:

$$R_{ha} = \frac{k_B \times T}{6 \times \pi \times \eta_s \times D_c}$$

where k B is the Boltzmann constant, T is the absolute temperature and η_s is the solvent viscosity.

The relative excess scattering intensity (Ir) was determined as the total intensity minus the solvent scattering divided by the scattering of toluene at 20 °C. Ir is related to the osmotic compressibility ($(d\pi/dC)^{-}1$) and the z average structure factor (S(q)):

$$Ir = K.C.R.T.(d\pi/dc)^{-1}S(q)$$

With R the gas constant and T the absolute temperature. In dilute solutions Ir is related to the weight average molar mass (Mw) and the z-average structure factor (S(q)):

$$Ir = K.C.Mw.S(q)$$

With C the solute concentration and K an optical constant that depends on the refractive index increment. S(q) describes the dependence of Ir on the scattering wave vector. For the concentrations studied (0.5 to 10 g/L), interactions influence the scattering intensity and the result obtained by extrapolation to q = 0 represents an apparent value for the apparent molar mass (M_a).

The weight percentage of the remaining flower-like aggregates in solution after plasma treatment is calculated according to equation (1):

$$C\ (\%) = \frac{Ma\ (APPJ)}{Ma\ (untreated)} \times 100 \quad (1)$$

The concentration of self-assembled tPEO chains in solution after plasma treatment can be obtained following equation (2):

$$C_{tPEO\text{-}APPJ\ (g/L)} = \left(\frac{Ma\ (APPJ)}{Ma\ (untreated)}\right) \times C_{(tPEO\ initial)}\ \left(g/L\right) \quad (2)$$

By this way, the concentration of the degraded flower-like aggregates can be deduced from equation (3):

$$C_{degraded}\ (g/L) = C_{tPEO\ initial} - C_{tPEO\text{-}APPJ}\ (g/L) \quad (3)$$

2.6. Rheology

Rheological measurements were done at 25 °C with a stress-control rheometer MCR301 (Anton Paar, Austria) using a cone-plate geometry (CP: 40 mm, gap: 1 mm). The measurements were done in the linear response regime (f = 1 Hz). For *in situ* photo-crosslinking, the sample was covered with mineral oil in order to avoid evaporation and the rheometer protected from light. A blue LED (Thorlabs – M450LP1) (λ_{max} = 450 nm) was equipped with a light guide (Ø = 5 mm) placed 5 cm below the glass plate. The samples were irradiated at ~ 0.1 W/cm^2 during 3 min.

2.7. ^1H NMR

Proton nuclear magnetic resonance (^{1}H NMR) with a Bruker Advance 400 MHz spectrometer was employed to characterize the triblock copolymer. The tPEO was dissolved in deuterated water at a concentration of 2 g/L and the ^{1}H NMR spectra was recorded at room temperature.

2.8. pH

The pH of the solutions was measured immediately after plasma treatment in 2 mL of solution using an MM 41 Crison multimeter with 50 28 probe (Crison, Spain).

3. Results

An atmospheric pressure plasma jet was employed to treat a Poly(2-methacryloyloxyethyl acrylate)-b-poly(ethylene oxide)-b-poly(2-methacryloyloxyethyl acrylate) triblock copolymer (tPEO) solution at the suitable concentration necessary to allow obtaining a self-standing hydrogel (40 g/L), and compared to PBS as control. A linear evaporation was observed during APPJ treatments (Fig. 3a) leading to up to 15% water evaporation after 15 min of APPJ treatment. The pH remained relatively stable in the polymer, with minor decrease of around 0.4 unit of pH only, after APPJ treatments (Fig. 3b).

To investigate the effects of plasma on the triblock copolymer and photo-crosslinked hydrogels, different concentrations of tPEO were treated by APPJ. The evolutions of the apparent molar mass (M_a) and apparent hydrodynamic radius (R_{ha}) of the tPEO self-assemblies in aqueous solution were measured by static (SLS) and dynamic (DLS) light scattering respectively as a function of APPJ treatment time and concentration (Fig. 4). The samples did not exhibit any angular dependence of the scattered intensity indicating that the scattering objects are small (Rg < 20 nm) (Fig. S1). APPJ treatment of a solution of tPEO flower-like micelles (at C = 0.5 g/L) revealed a clear decrease of M_a after APPJ treatments up to 900 s (Fig. 4a). The influence of the polymer concentration on the self-assembly of the flower-like micelles was investigated up to C = 10 g/L at the longest APPJ treatment time studied here (t = 900 s). The M_a of each sample was measured just after APPJ treatment and 24 h later (Fig. 4b). No time evolution of the plasma-treated samples was observed after 24 h. As previously reported [31], increasing the concentration leads to the formation of larger aggregates due to bridging of micelles. APPJ treatment led to a decrease of M_a whatever the initial tPEO concentration. This phenomenon could be attributed to the degradation of tPEO micellar aggregates whose number or aggregation number (*i.e.* number of polymeric chains per micelle) decreases with the plasma treatment. Yet, the hydrodynamic radius (R_{ha}) of the aggregates slightly increases after 15 min of APPJ treatment (Fig. 4c). The total amount of degraded material being almost constant whatever the initial concentration, the degradation effect due to plasma is very important at low polymer concentration but negligible at high concentration (Fig. 4d).

The effects of APPJ on the properties of tPEO solutions were further investigated by rheology at concentrations were tPEO forms dynamic physical hydrogels [31]. The viscosity of the tPEO solution at C = 40 g/L (without photo-initiator system (PIS)) was evaluated at different APPJ treatment times (Fig. 5a). The untreated solution initially exhibited a Newtonian behavior up to a shear rate $\dot{\gamma} = 100\ s^{-1}$ with a viscosity of η = 0.34 Pa.s. By increasing the APPJ treatment time, an increase of the viscosity was progressively observed.

As described earlier, there is an evaporation of 1%/min in the tPEO solution due to the gas flow during APPJ treatment. Thus, the viscosity of a tPEO solution treated for 15 min was compared to an untreated tPEO solution at C = 47 g/L; concentration reached after 15 min of APPJ treatment. A slight decrease of the zero-shear viscosity of the APPJ-treated tPEO was observed compared to an untreated solution at 47 g/L. In parallel, the same comparison was made with tPEO solutions containing the PIS (Fig. 5b). A non-Newtonian fluid of high zero shear viscosity was obtained by treating the solution during 15 min by APPJ, in contrast to the untreated solutions at C = 40 g/L and C = 47 g/L.

Higher storage (G′) and loss (G″) moduli were obtained for the APPJ-treated solution compared to the untreated one (Fig. 6a). Moreover, at low frequency, the 15 min APPJ-treated sample tends to a very soft solid behavior (G′ > G″). Fig. 6b represents the evolution of G' and G" during *in situ* photo-crosslinking of the hydrogel. After 30 s, samples were exposed to blue light during 3 min. Faster crosslinking and higher elastic modulus were observed for the APPJ-treated hydrogel. Fig. 6c shows the frequency dependence of the moduli for the photo-crosslinked hydrogels. Both untreated and APPJ-treated photo-cross-linked hydrogels exhibit a plateau for G′(ω) at low frequency indicating a soft solid behavior. However, the elastic modulus of the APPJ-treated hydrogel obtained after photo irradiation was twice as high as that of the untreated one indicating a higher extent of cross-linking. After APPJ treatment, photo-cross-linked hydrogels were more brittle than the untreated one as shown by their lower strain at breakage (Fig. 6d).

To further investigate the structural changes in the structure of the tPEO, ^{1}H NMR experiments were performed at 2 g/L after 15 min of plasma treatment in D_2O (Fig. 7).

^{1}HNMR analysis shows degradation of some PEO chains and that the

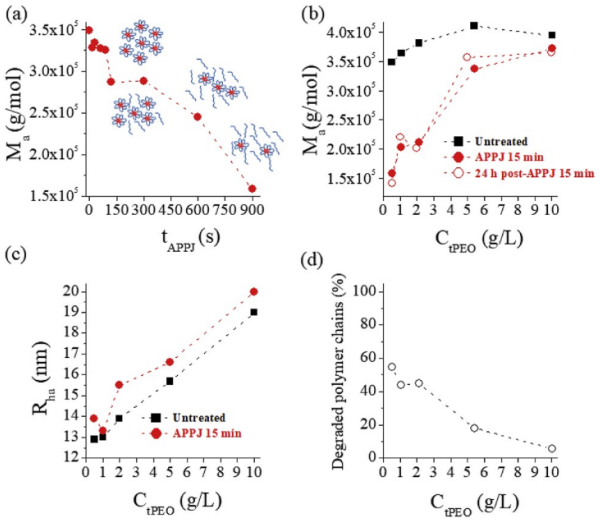

Fig. 4. (a): Apparent molar mass (M_a) of tPEO at C = 0.5 g/L as a function of the APPJ treatment time. (b): M_a as a function of tPEO concentration before APPJ treatment (squares), after 15 min of APPJ (filled circles) and 24 h later (empty circles). (c): Apparent hydrodynamic radius (R_{ha}) of the micelles as a function of tPEO concentration before APPJ treatment (squares) and after 15 min of APPJ (circles). (d): Percentage of the tPEO micellar aggregates degraded after 15 min of APPJ treatment as a function of the initial tPEO concentration.

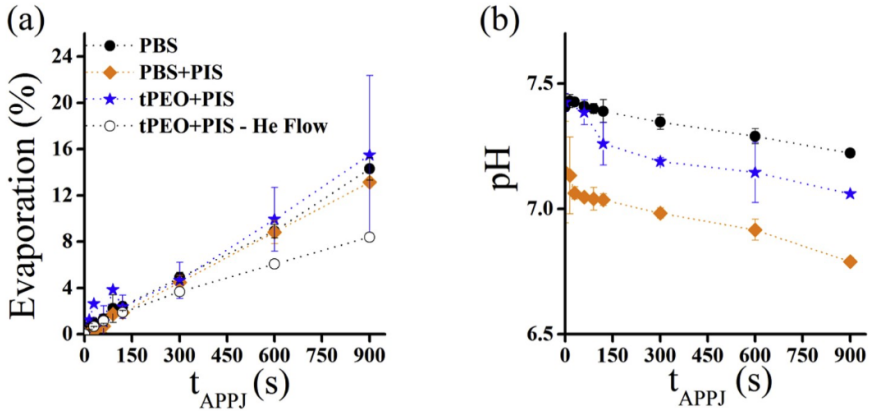

Fig. 3. Effect of APPJ treatment time on the tPEO polymer (with the photo-initiator system (PIS)) on (a): Evaporation and (b) pH. PBS was used as control and in (a) the polymer solution was subjected to gas flow alone without plasma treatment.

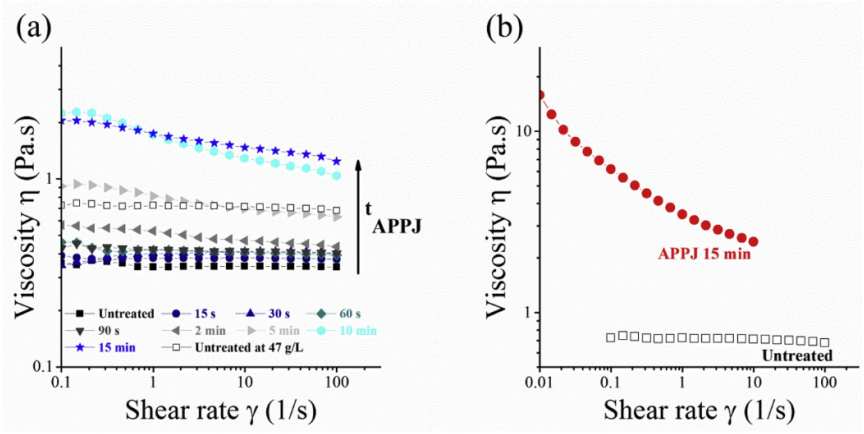

Fig. 5. (a): Viscosity of tPEO solution at C = 40 g/L for different APPJ treatment times and an untreated at C = 47 g/L. (b): Viscosity of a 15 min APPJ-treated tPEO solution at C = 40 g/L (red dots) compared to untreated one at C = 47 g/L (empty black squares) in the presence of the PIS.

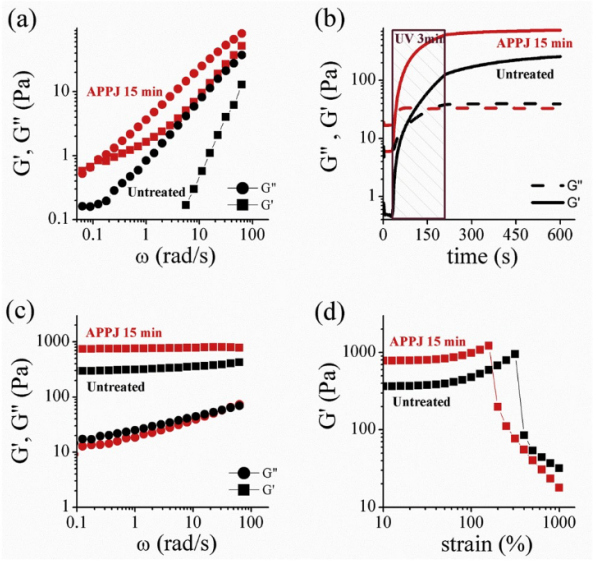

Fig. 6. (a): Frequency dependence of the shear moduli of a 15 min APPJ-treated (red) and untreated tPEO at C = 47 g/L in the presence of the PIS (black). (b): Time evolution of the moduli of a 15 min APPJ-treated tPEO solution at C = 40 g/L (red) and an untreated tPEO solution at C = 47 g/L (black). Light irradiation was switched on after 30 s and stopped 3 min after (c): Frequency dependence of the shear moduli of a 15 min APPJ-treated tPEO hydrogel (red) compared to an untreated one (black) after photo-cross-linking. (d): Evolution of the storage modulus with strain for a 15 min APPJ-treated tPEO photo-cross-linked hydrogel at C = 40 g/L compared to an untreated one at C = 47 g/L (black).

PMEA hydrophobic block is also affected by the plasma treatment. In fact, by setting the integration of the CH_2 peak of the PEO to 1080 (DP_n = 270), it was observed that the integration of the characteristic signals of the PMEA block decrease by a factor of ~2. However, all the signals do not decrease at the same rate. The characteristic peaks of the methacrylate double bonds decrease more than the methyl signals (a, a') at 1.2 ppm. This indicates that plasma treatment also induces a cross-linking of the double bonds.

4. Discussion

The effects of a He APPJ treatment were investigated here on tPEO solutions able to form hydrogels (Fig. 1), with the aim of understanding the potential chemical and physical modifications of such kind of polymeric systems in solution.

The plasma gas chemistry of the APPJ employed here includes $O^{\bullet}$ radicals, N_2 1^{st} positive and N_2^+ 2^{nd} negative and He, among other reactive species [41]. These species can react with the treated liquid (water, saline solutions or cell culture media) and after diffusion and cascade reactions they produce short-lived species able to recombine into chemically stable species, including nitrates, nitrites, hydrogen peroxides, among others; [25,42–47], depending on the chemical composition of the treated-liquid [45,48,49]. Despite this, the effects of diffusion and reaction of these RONS in polymer chains in solution are a complex issue and largely unexplored.

The gas flow and distance to the solution employed here were selected according to previous works as they maximize the production of RONS in a liquid [50], and will thus allow to investigate any potential modifications in the polymer solution.

It is well established that evaporation occurs in liquids during plasma treatment. The evaporation depends on the plasma device employed and is mainly related to the gas flow which is directly applied on the surface of the liquid [51,52]. To confirm that, tPEO + PIS solutions were treated without plasma only using the He gas flow and a linear evaporation up to 9% was recorded. This value is slightly below than that recorded after plasma treatment (about 15%). It can therefore be assumed that the main contribution to evaporation is mainly due to the gas flow with an additional contribution derived from the plasma treatment itself. As there is no heating of the polymer solution due to plasma treatment (only 4 °C increase in 15 min plasma treatment was recorded), this is not a parameter expected to contribute significantly to evaporation. The linear increase of the evaporation observed in Fig. 3a following plasma treatment was in agreement with observations in polymers dissolved in organic solvents for electrospinning applications [12,13].

It is well-known that the chemical composition of the plasma treated-liquids have a major impact on the generation of reactive species and therefore on its pH variations [52–54], most of the reported studies showing an acidification after plasma exposure [45,52,55–58]. This acidification has been widely described as being induced by the accumulation of the reactive species, especially NO_2^- and NO_3^- generated in solution from the APPJ. In the present work, pH of PBS, tPEO and PBS + PIS used for tPEO photo-crosslinking remained between 6.5 and 7.5 (Fig. 3b) and showed a very limited acidification. By avoiding the acidification of the solution, pH buffering prevents potential subsequent reactions of the two main species usually detected, H_2O_2 and NO_2, for example, to form peroxynitric acid (ONOOOH).

The effect of APPJ treatment on the self-assembly and rheological

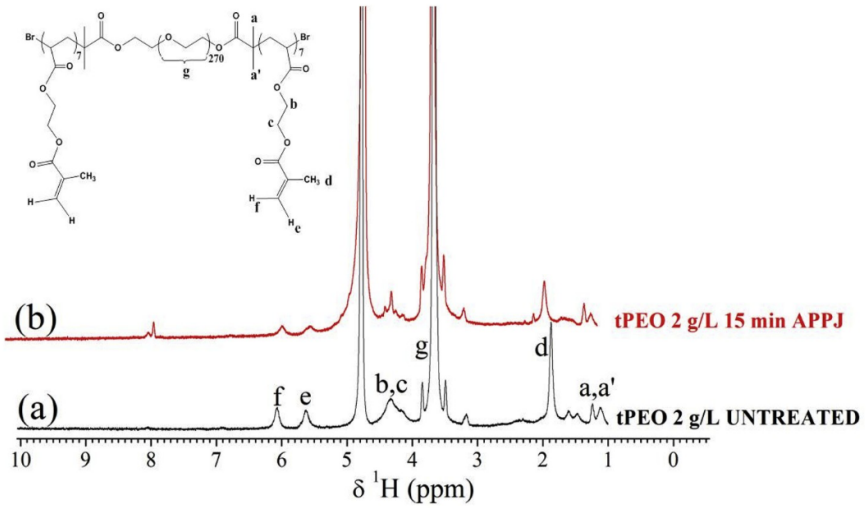

Fig. 7. ^{1}H NMR spectra (400 MHz, in D_2O) of (a) untreated tPEO, (b) 15 min APPJ-treated tPEO at 2 g/L in D_2O.

behaviour of tPEO solutions was investigated here by different techniques. The self-assembling colloidal nature of the selected polymer allowed using static (SLS) and dynamic (DLS) light scattering to quantify the evolution of size (R_{ha}) and apparent molar mass (M_a) of the amphiphilic tPEO self-assemblies in aqueous solution (Fig. 4). On tPEO single micelle solutions (at C = 0.5 g/L), a decrease of the apparent molar mass with APPJ treatment time was observed. This decrease cannot be attributed to the solvent evaporation since concentrating the solution would lead to higher M_a. Two scenarios are thus possible: 1) The number of micelles remains constant but their molar mass decreases or 2) the average molar mass of the micelles remains constant but their number decreases. By analyzing the evolution of the micelles size (Fig. 4c), we observe that the size of the micelles has slightly increased after APPJ treatment. As the radius of star-like objects (including flower-like micelles) varies with the aggregation number (N_{agg}) as $R \sim N_{agg}^{1/5}$ [59], a decrease of N_{agg} should lead to a decrease of R_{ha}. So, it can be concluded that scenario 1 is not occurring. The conclusion is therefore that the micelles size is barely affected but the total number of micelles decreases by destruction of part of the block copolymer chains under plasma treatment. The broken chains are not able to self-assemble anymore and remain as unimers in solution; their scattering intensity is thus negligible compared to the intensity scattered by the micelles. Simultaneously, because they are dynamic, the micelles reorganize to recover their equilibrium structure (with a constant N_{agg}) which barely depends on the concentration in diluted regime [31,39]. This observation can be done for all the tPEO concentrations studied. This scenario is illustrated in Fig. 8.

The slight increase of R_{ha} can be attributed to a partial covalent crosslinking of the micelles due to the reactive species or radicals generated by the plasma treatment. This observation is supported by ^{1}HNMR where the decrease of the methacrylate peaks at δ = 5.6 and 6.1 ppm indicates a partial crosslinking of the PMEA group (Fig. 7). This hypothesis was also confirmed by the rheological measurements made on concentrated tPEO solutions (Fig. 5).

To produce photo-cross-linked hydrogels that can be handled, the polymer solution concentration must be far above the percolation concentration (Cp ≈ 20 g/L). A rheological study was thus made with a tPEO concentration of 40 g/L. A progressive increase of the tPEO solution viscosity was observed with increasing APPJ treatment time (Fig. 5a). Concomitantly, a non-Newtonian behavior appears from shear rates of 0.2–0.3 s^{-1}. As it was shown that water evaporation occurred during the plasma treatment (Fig. 3a), the viscosity increase can partly be explained by the concentration of the tPEO solution. Anyhow, at the same time, the plasma treatment also degrades polymeric chains which are not able to self-assemble anymore and thus reduces the connectivity of the transient polymeric network. For instance, the hydrophilic PEO block might be slightly affected by APPJ treatment since the plasma-treated precursor alone shows some degradation of the main chains (only detectable at low concentration) (Fig. S3) and a partial crosslinking (Fig. S4 and Table S1). Moreover, the signal appearing in APPJ-treated tPEO at δ = 8.15 ppm that could be attributed to a small molecule such as formic acid [60] which could be derived from some

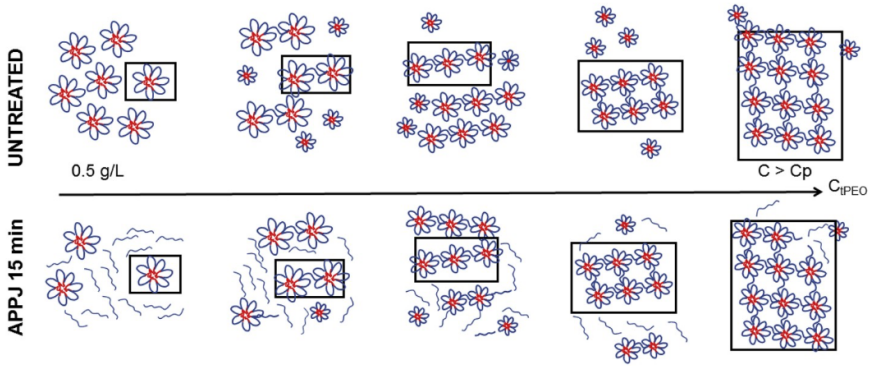

Fig. 8. Schematic representation of the effect of concentration and plasma treatment on tPEO micellar solutions.

potential reactions between the degraded tPEO and reactive species generated by APPJ in the polymer solution [15].

The chemical modifications of the PMEA hydrophobic block of the polymer by the plasma treatment (Fig. 7), which lead to the irreversible cross-linking of a small fraction of the micellar aggregates, contribute to increase the viscosity of the solution. The evolution of the rheological behavior is thus a complex combination of these 3 factors: 1) solvent evaporation, 2) block copolymer chains degradation, 3) partial irreversible cross-linking. By comparing the rheological behaviour of the APPJ treated solution and a non-treated solution at C = 47 g/L (concentration reached after plasma treatment), it can be concluded that the irreversible cross-linking affects more the properties than polymeric chains degradation since the zero-shear viscosity of the APPJ-treated solution is higher than that of the tPEO solution at C = 47 g/L.

In the presence of PIS, APPJ-treated tPEO solution exhibits a non-Newtonian fluid behavior and a solid-like behavior appears at low frequency (G' > G'') (Figs. 5b and 6a). These results indicate that a very soft (G' < 1 Pa) and fragile hydrogel is formed by treating the polymeric solution by APPJ during 15 min. The hydrogel formed during this process is probably continuously broken by the shear applied to measure the viscosity which could explain the non-Newtonian behavior. It must be pointed out that the partial linkage of micellar aggregates induced by APPJ treatment in the absence of PIS does not lead to the formation of soft hydrogel (Fig. S3). The presence of the PIS in solution probably leads to the creation of higher amount of radicals in solution under APPJ treatment either because of the UV-VIS light emitted by the plasma or by the interaction between the plasma and the PIS. Nevertheless, the tPEO solution is still able to flow so it can potentially be injected. Furthermore, the photo-crosslinking is faster and more efficient indicating that the integrity of both PIS and polymeric micelles remain sufficiently high to allow for the formation of covalent hydrogels. As shown in Fig. 6c, this pre-cross-linking induced by APPJ treatment is beneficial to the material since the elastic modulus obtained after photo-cross-linking is twice as higher than that measured on untreated hydrogels after the same irradiation time. The counterpart to this higher extent of cross-linking is that the hydrogels formed are more fragile; they break at lower stretching rates (Fig. 6d). As the different applications of APPJ treated hydrogels investigated up to now [15,17,18,61] are not intended for load-bearing applications, this would not seem to be a restriction for future use.

5. Conclusion

The effects of atmospheric pressure plasma treatments of an amphiphilic poly (ethylene glycol)-based triblock copolymer solution were investigated here. In this work, plasma treatment led to the irreversible degradation of a small amount of the block copolymer chains, through their hydrophobic block. This treatment had a non-negligible effect on the self-assembled structures at low polymer concentrations but it only slightly modified the properties of the transient polymeric network at high concentration. In presence of a photo-initiating system, plasma treatment alone induced a slight cross-linking leading to a very weak and fragile hydrogel, which could be efficiently and rapidly covalently cross-linked under visible light irradiation. The pre-cross-linking induced by the plasma helped in reaching higher mechanical properties than that obtained with untreated hydrogels. Overall, this work opens new perspectives for further applications in plasma-treated hydrogels for several biomedical applications.

Declaration of competing interest

The authors declare that they have no known competing financial interests or personal relationships that could have appeared to influence the work reported in this paper.

CRediT authorship contribution statement

Inès Hamouda: Formal analysis, Investigation, Methodology, Writing - original draft. **Cédric Labay:** Formal analysis, Investigation, Methodology, Supervision, Validation, Writing - review & editing. **Maria Pau Ginebra:** Funding acquisition, Methodology, Supervision, Writing - review & editing. **Erwan Nicol:** Formal analysis, Investigation, Methodology, Writing - original draft. **Cristina Canal:** Conceptualization, Funding acquisition, Methodology, Project administration, Supervision, Writing - review & editing.

Acknowledgements

This project has received funding from the European Research Council (ERC) under the European Union's Horizon 2020 research and innovation program (Grant agreement No714793) and the financial support of MAT2015-65601-R project (MINECO/FEDER, EU), and of Generalitat de Catalunya for the 2017 SGR 1165. MPG acknowledges the ICREA Academia award from the Generalitat de Catalunya.

Appendix A. Supplementary data

Supplementary data to this article can be found online at https://doi.org/10.1016/j.polymer.2020.122308.

References

[1] C. Canal, R. Molina, E. Bertran, P. Erra, Wettability, ageing and recovery process of plasma-treated polyamide 6, J. Adhes. Sci. Technol. 18 (2004) 1077–1089.
[2] A. Fridman, Plasma Chemistry, Cambridge university Press, New York, USA, 2008.
[3] E. Stoffels, I.E. Kieft, R.E.J. Sladek, L.J.M. van den Bedem, E.P. van der Laan, M. Steinbuch, Plasma needle for in vivo medical treatment: recent developments and perspectives, Plasma Sources Sci. Technol. 15 (2006) S169–S180.
[4] J.F. Kolb, A.-A.H. Mohamed, R.O. Price, R.J. Swanson, A. Bowman, R.L. Chiavarini, M. Stacey, K.H. Schoenbach, Cold atmospheric pressure air plasma jet for medical applications, Appl. Phys. Lett. 92 (2008) 241501.
[5] X. Lu, Z. Xiong, F. Zhao, Y. Xian, Q. Xiong, W. Gong, C. Zou, Z. Jiang, Y. Pan, A simple atmospheric pressure room-temperature air plasma needle device for biomedical applications, Appl. Phys. Lett. 95 (2009) 181501.
[6] D.B. Graves, Low temperature plasma biomedicine: a tutorial review, Phys. Plasmas 21 (2014) 80901.
[7] K.-D. Weltmann, M. Polak, K. Masur, T. von Woedtke, J. Winter, S. Reuter, Plasma processes and plasma sources in medicine, Contrib. Plasma Phys. 52 (2012) 644–654.
[8] S.K. Pankaj, K.M. Keener, Cold plasma: background, applications and current trends, Curr. Opin. Food Sci. 16 (2017) 49–52.
[9] M. Laroussi, X. Lu, Room-temperature atmospheric pressure plasma plume for biomedical applications, Appl. Phys. Lett. 87 (2005) 113902.
[10] J. Winter, R. Brandenburg, K.-D. Weltmann, Atmospheric pressure plasma jets: an overview of devices and new directions, Plasma Sources Sci. Technol. 24 (2015) 64001.
[11] H. Tanaka, K. Ishikawa, M. Mizuno, S. Toyokuni, H. Kajiyama, F. Kikkawa, H.-R. Metelmann, M. Hori, State of the art in medical applications using non-thermal atmospheric pressure plasma, Rev. Mod. Plasma Phys. 1 (2017) 3.
[12] S. Grande, P. Cools, M. Asadian, J. Van Guyse, I. Onyshchenko, H. Declercq, R. Morent, R. Hoogenboom, N. De Geyter, Fabrication of PEOT/PBT nanofibers by atmospheric pressure plasma jet treatment of electrospinning solutions for tissue engineering, Macromol. Biosci. (2018) 1800309.
[13] S. Grande, J. Van Guyse, A.Y. Nikiforov, I. Onyshchenko, M. Asadian, R. Morent, R. Hoogenboom, N. De Geyter, Atmospheric pressure plasma jet treatment of poly-ε-caprolactone polymer solutions to improve electrospinning, ACS Appl. Mater. Interfaces 9 (2017) 33080–33090.
[14] Q. Shi, N. Vitchuli, J. Nowak, Z. Lin, B. Guo, M. Mccord, M. Bourham, X. Zhang, Atmospheric plasma treatment of pre-electrospinning polymer solution: a feasible method to improve electrospinnability, J. Polym. Sci., Part B: Polym. Phys. 49 (2011) 115–122.
[15] C. Labay, I. Hamouda, F. Tampieri, M.P. Ginebra, C. Canal, Production of reactive species in alginate hydrogels for cold atmospheric plasma-based therapies, Sci. Rep. 9 (2019).
[16] E.J. Szili, J.-S. Oh, S.-H. Hong, A. Hatta, R.D. Short, Probing the transport of plasma-generated RONS in an agarose target as surrogate for real tissue: dependency on time, distance and material composition, J. Phys. D Appl. Phys. 48 (2015) 202001.
[17] E.J. Szili, S.H. Hong, J.S. Oh, N. Gaur, R.D. Short, Tracking the penetration of plasma reactive species in tissue models, Trends Biotechnol. (2017).
[18] J.-S. Oh, E.J. Szili, N. Gaur, S.-H. Hong, H. Furuta, H. Kurita, A. Mizuno, A. Hatta, R.D. Short, How to assess the plasma delivery of RONS into tissue fluid and tissue, J. Phys. D Appl. Phys. 49 (2016).

[19] H.-R. Metelmann, C. Seebauer, V. Miller, A. Fridman, G. Bauer, D.B. Graves, J.-M. Pouvesle, R. Rutkowski, M. Schuster, S. Bekeschus, et al., Clinical experience with cold plasma in the treatment of locally advanced head and neck cancer, Clin. Plasma Med. (2017).

[20] K.-D. Weltmann, M. Polak, K. Masur, T. von Woedtke, J. Winter, S. Reuter, Plasma processes and plasma sources in medicine, Contrib. Plasma Phys. 52 (2012) 644–654.

[21] K.-D. Weltmann, E. Kindel, R. Brandenburg, C. Meyer, R. Bussiahn, C. Wilke, T. von Woedtke, Atmospheric pressure plasma jet for medical therapy: plasma parameters and risk estimation, Contrib. Plasma Phys. 49 (2009) 631–640.

[22] G. Bauer, D.B. Graves, Mechanisms of selective antitumor action of cold atmospheric plasma-derived reactive oxygen and nitrogen species, Plasma Process. Polym. 13 (2016) 1157–1178.

[23] D.B. Graves, Reactive species from cold atmospheric plasma: implications for cancer therapy, Plasma Process. Polym. 11 (2014) 1120–1127.

[24] D.B. Graves, Reactive species from cold atmospheric plasma: implications for cancer therapy, Plasma Process. Polym. 11 (2014) 1120–1127.

[25] A. Khlyustova, C. Labay, Z. Machala, M.-P. Ginebra, C. Canal, Important parameters in plasma jets for the production of RONS in liquids for plasma medicine: a brief review, Front. Chem. Sci. Eng. 13 (2019) 238–252.

[26] C.-C. Lin, K.S. Anseth, PEG hydrogels for the controlled release of biomolecules in regenerative medicine, Pharm. Res. (N. Y.) 26 (2009) 631–643.

[27] J.A. Burdick, K.S. Anseth, Photoencapsulation of osteoblasts in injectable RGD-modified PEG hydrogels for bone tissue engineering, Biomaterials 23 (2002) 4315–4323.

[28] P.J. LeValley, M.W. Tibbitt, B. Noren, P. Kharkar, A.M. Kloxin, K.S. Anseth, M. Toner, J. Oakey, Immunofunctional photodegradable poly(ethylene glycol) hydrogel surfaces for the capture and release of rare cells, Colloids Surf. B Biointerfaces 174 (2019) 483–492.

[29] N.A. Peppas, K.B. Keys, M. Torres-Lugo, A.M. Lowman, Poly(ethylene glycol)-containing hydrogels in drug delivery, J. Contr. Release 62 (1999) 81–87.

[30] P. Colombo, R. Bettini, N.A. Peppas, Observation of swelling process and diffusion front position during swelling in hydroxypropyl methyl cellulose (HPMC) matrices containing a soluble drug, J. Contr. Release 61 (1999) 83–91.

[31] V. Kadam, T. Nicolai, E. Nicol, L. Benyahia, Structure and rheology of self-assembled telechelic associative polymers in aqueous solution before and after photo-cross-linking, Macromolecules 44 (2011) 8225–8232.

[32] G. Chen, N. Kawazoe, Y. Ito, Photo-crosslinkable hydrogels for tissue engineering applications, in: Photochemistry for Biomedical Applications, Springer Singapore, Singapore, 2018, pp. 277–300.

[33] B.D. Fairbanks, M.P. Schwartz, C.N. Bowman, K.S. Anseth, Photoinitiated polymerization of PEG-diacrylate with lithium phenyl-2,4,6-trimethylbenzoylphosphinate: polymerization rate and cytocompatibility, Biomaterials 30 (2009) 6702–6707.

[34] J.L. Ifkovits, J.A. Burdick, Review: photopolymerizable and degradable biomaterials for tissue engineering applications, Tissue Eng. 13 (2007) 2369–2385.

[35] J.A. Killion, L.M. Geever, D.M. Devine, L. Grehan, J.E. Kennedy, C. L. Higginbotham, Modulating the mechanical properties of photopolymerised polyethylene glycol–polypropylene glycol hydrogels for bone regeneration, J. Mater. Sci. 47 (2012) 6577–6585.

[36] A. Klymenko, T. Nicolai, C. Chassenieux, O. Colombani, E. Nicol, Formation of porous hydrogels by self-assembly of photo-cross-linkable triblock copolymers in the presence of homopolymers, Polymer 106 (2016) 152–158.

[37] A. Klymenko, T. Nicolai, L. Benyahia, C. Chassenieux, O. Colombani, E. Nicol, Multiresponsive hydrogels formed by interpenetrated self-assembled polymer networks, Macromolecules 47 (2014) 8386–8393.

[38] E. Nicol, T. Nicolai, J. Zhao, T. Narita, Photo-cross-linked self-assembled poly (ethylene oxide)-based hydrogels containing hybrid junctions with dynamic and permanent cross-links, ACS Macro Lett. 7 (2018) 683–687.

[39] V.S. Kadam, E. Nicol, C. Gaillard, Synthesis of flower-like poly(ethylene oxide) based macromolecular architectures by photo-cross-linking of block copolymers self-assemblies, Macromolecules 45 (2012) 410–419.

[40] R. Zaplotnik, M. Bišćan, Z. Kregar, U. Cvelbar, M. Mozetič, S. Milošević, Influence of a sample surface on single electrode atmospheric plasma jet parameters, Spectrochim. Acta Part B At. Spectrosc. 103–104 (2015) 124–130.

[41] C. Canal, R. Fontelo, I. Hamouda, J. Guillem-Marti, U. Cvelbar, M.-P. Ginebra, Plasma-induced selectivity in bone cancer cells death, Free Radic. Biol. Med. 110 (2017).

[42] T. Adachi, H. Tanaka, S. Nonomura, H. Hara, S.I. Kondo, M. Hori, Plasma-activated medium induces A549 cell injury via a spiral apoptotic cascade involving the mitochondrial-nuclear network, Free Radic. Biol. Med. 79 (2015).

[43] S. Mohades, M. Laroussi, V. Maruthamuthu, Moderate plasma activated media suppresses proliferation and migration of MDCK epithelial cells, J. Phys. D Appl. Phys. 50 (2017) 185205.

[44] D. Yan, H. Cui, W. Zhu, A. Talbot, L.G. Zhang, J.H. Sherman, M. Keidar, The strong cell-based hydrogen peroxide generation triggered by cold atmospheric plasma, Sci. Rep. 7 (2017) 10831.

[45] P.J. Bruggeman, M.J. Kushner, B.R. Locke, J.G.E. Gardeniers, W.G. Graham, D. B. Graves, R.C.H.M. Hofman-Caris, D. Maric, J.P. Reid, E. Ceriani, et al., Plasma–liquid interactions: a review and roadmap, Plasma Sources Sci. Technol. 25 (2016) 53002.

[46] A. Lin, Y. Gorbanev, J. De Backer, J. Van Loenhout, W. Van Boxem, F. Lemière, P. Cos, S. Dewilde, E. Smits, A. Bogaerts, Non-Thermal plasma as a unique delivery system of short-lived reactive oxygen and nitrogen species for immunogenic cell death in melanoma cells, Adv. Sci. 6 (2019) 1802062.

[47] Y. Gorbanev, D. O'Connell, V. Chechik, Non-Thermal plasma in contact with water: the origin of species, Chem. Eur J. 22 (2016).

[48] D. Yan, H. Cui, W. Zhu, N. Nourmohammadi, J. Milberg, L.G. Zhang, J.H. Sherman, M. Keidar, The specific vulnerabilities of cancer cells to the cold atmospheric plasma-stimulated solutions, Sci. Rep. 7 (2017) 4479.

[49] S.A. Norberg, W. Tian, E. Johnsen, M.J. Kushner, Atmospheric pressure plasma jets interacting with liquid covered tissue: touching and not-touching the liquid, J. Phys. D Appl. Phys. 47 (2014).

[50] J. Tornin, M. Mateu-Sanz, A. Rodríguez, C. Labay, R. Rodríguez, C. Canal, Pyruvate plays a main role in the antitumoral selectivity of cold atmospheric plasma in osteosarcoma, Sci. Rep. 9 (2019).

[51] S. Ikawa, K. Kitano, S. Hamaguchi, Effects of pH on bacterial inactivation in aqueous solutions due to low-temperature atmospheric pressure plasma application, Plasma Process. Polym. 7 (2010) 33–42.

[52] F. Girard, V. Badets, S. Blanc, K. Gazeli, L. Marlin, L. Authier, P. Svarnas, N. Sojic, F. Clément, S. Arbault, Formation of reactive nitrogen species including peroxynitrite in physiological buffer exposed to cold atmospheric plasma, RSC Adv. 6 (2016) 78457–78467.

[53] J. Chauvin, F. Judée, M. Yousfi, P. Vicendo, N. Merbahi, Analysis of reactive oxygen and nitrogen species generated in three liquid media by low temperature helium plasma jet, Sci. Rep. 7 (2017) 4562.

[54] S. Ikawa, K. Kitano, S. Hamaguchi, Effects of pH on bacterial inactivation in aqueous solutions due to low-temperature atmospheric pressure plasma application, Plasma Process. Polym. 7 (2010) 33–42.

[55] Z. Machala, B. Tarabova, K. Hensel, E. Spetlikova, L. Sikurova, P. Lukes, formation of ROS and RNS in water electro-sprayed through transient spark discharge in air and their bactericidal effects, Plasma Process. Polym. 10 (2013) 649–659.

[56] S. Samukawa, M. Hori, S. Rauf, K. Tachibana, P. Bruggeman, G. Kroesen, J. C. Whitehead, A.B. Murphy, A.F. Gutsol, S. Starikovskaia, et al., The 2012 plasma roadmap, J. Phys. D Appl. Phys. 45 (2012) 253001.

[57] I. Adamovich, S.D. Baalrud, A. Bogaerts, P.J. Bruggeman, M. Cappelli, V. Colombo, U. Czarnetzki, U. Ebert, J.G. Eden, P. Favia, et al., The 2017 Plasma Roadmap: low temperature plasma science and technology, J. Phys. D Appl. Phys. 50 (2017) 323001.

[58] P.J. Bruggeman, M.J. Kushner, B.R. Locke, J.G.E. Gardeniers, W.G. Graham, D. B. Graves, R.C.H.M. Hofman-Caris, D. Maric, J.P. Reid, E. Ceriani, et al., Plasma–liquid interactions: a review and roadmap, Plasma Sources Sci. Technol. 25 (2016) 53002.

[59] M. Daoud, J.P. Cotton, Star shaped polymers : a model for the conformation and its concentration dependence, J. Phys. 43 (1982) 531–538.

[60] K. Yoshida, C. Wakai, N. Matubayasi, M. Nakahara, NMR spectroscopic evidence for an intermediate of formic acid in the Water−Gas−Shift reaction, J. Phys. Chem. 108 (2004) 7479–7482.

[61] J.S. Endre, W.B. James, D.S. Robert, A 'tissue model' to study the plasma delivery of reactive oxygen species, J. Phys. D Appl. Phys. 47 (2014) 152002.